
EGOR: Efficient Generated Objects Replay for incremental object detection

Zijia An, Boyu Diao,* Libo Huang, Ruiqi Liu, Zhulin An, Yongjun Xu
Institute of Computing Technology, Chinese Academy of Sciences
{anzijia23p, diaoboyu2012, anzhulin, xyj}@ict.ac.cn, www.huanglibo@gmail.com,
liuruiqi23@mails.ucas.ac.cn

Abstract

Incremental object detection aims to simultaneously maintain old-class accuracy and detect emerging new-class objects in incremental data. Most existing distillation-based methods underperform when unlabeled old-class objects are absent in the incremental dataset. While the absence can be mitigated by generating old-class samples, it also incurs high computational costs. In this paper, we argue that the extra computational cost stems from the inconsistency between the detector and the generative model, along with redundant generation. To overcome this problem, we propose Efficient Generated Object Replay (EGOR). Specifically, we generate old-class samples by inverting the original detectors, thus eliminating the necessity of training and storing additional generative models. We also propose augmented replay to reuse the objects in generated samples, thereby reducing the redundant generation. In addition, we propose high-response knowledge distillation focusing on the knowledge related to the old class, which transfers the knowledge in generated objects to the incremental detector. With the addition of the generated objects and losses, we observe a bias towards old classes in the detector. We balance the losses for old and new classes to alleviate the bias, thereby increasing the overall detection accuracy. Extensive experiments conducted on MS COCO 2017 demonstrate that our method can efficiently improve detection performance in the absence of old-class objects.

1 Introduction

Modern target detectors [37] have achieved incredible performance on pre-defined datasets with fixed categories. However, in real-world scenarios with emerging new-class objects, fine-tuning the detector while fitting it to the new-class objects leads to severe performance degradation on the old-class objects [10], known as catastrophic forgetting [31]. Since unlabeled old-class objects and labeled new-class objects may co-occur in incremental data, some existing methods utilize the unlabeled old-class objects to mitigate catastrophic forgetting. However, the absence of old-class objects in incremental data is more general in real scenarios. Although the absence can be mitigated by generating old-class samples, the extra generation requires significant computational cost [34], thus limiting practical applications. Therefore, it is necessary to investigate efficient incremental object detection (IOD) for scenarios without old-class objects.

Existing IOD methods can be classified into distillation-based, parameter-restriction-based, and replay-based [25]. Most IOD methods are distillation-based [30, 16, 26, 8, 1, 7], transferring the old-class knowledge from the original detector to the incremental detector using distillation to regularize the model's outputs/features. However, the effectiveness of such methods depends on the presence of the old-class objects in the incremental data. Without the unlabeled old-class objects, the performance

*Corresponding Author.

of distillation-based methods degrades due to the absence of old-class information. In reality, due to the sparsity or irrelevance of the objects, non co-occurring scenes are more general, i.e., the captured image does not guarantee the simultaneous appearance of both old and new class objects, as shown in Fig.1a. Notably the co-occurring phenomenon only occurs in IOD and does not exist in the incremental classification task.

To better demonstrate the dependence of the old-class objects in the distillation-based approach, we compare the old-class accuracy in co-occurring and non co-occurring scenarios. The experimental results are shown in Fig.1b. The old-class accuracy substantially decreases when the old-class object is absent in the incremental dataset, which indicates that the existing distillation-based method’s performance depends on the presence of old-class objects and is unstable when apply in real-world scenarios. Previous work [34, 4] proposes to compensate for the absence of old class objects by generating old-class samples. These methods incorporate extra generative models to generate old-class samples. However, generative models require additional training before incremental learning, which incurs extra training costs. Moreover, these methods constantly generate samples throughout the incremental training period, incurring significant generation costs. The additional computational cost limits these methods when applied to real-world scenarios.

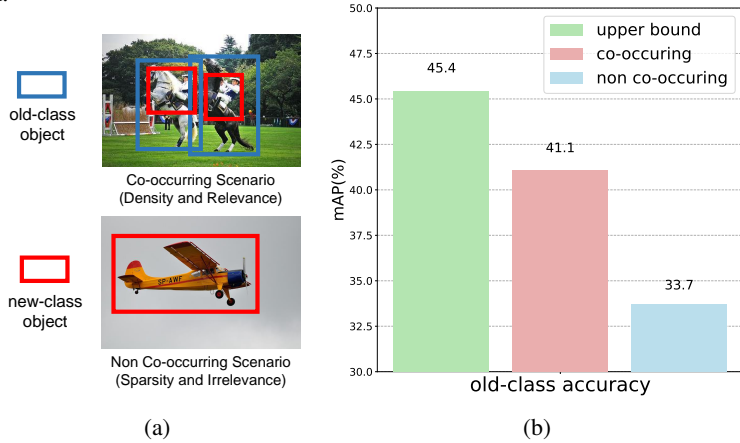


Figure 1: Co-occurring and non co-occurring scenarios.(a): We demonstrate that sparsity and irrelevance lead to a non co-occurring scenario. (b): Old-class accuracy in co-occurring and non co-occurring scenarios. We add the distillation to the GFL [17] baseline detector and conduct experiments on the MS COCO 2017 [21] dataset. In the experiments, we take the first 40 classes as old-class objects and the last 40 as new-class objects. Some images contain both old and new class objects. In the non co-occurring scenario, we only divide these images into the original dataset. In the co-occurring scenario, we divide these images into both the original dataset and the incremental dataset.

To mitigate catastrophic forgetting for non co-occurring IOD with low costs, we propose the Efficient Generated Objects Replay (EGOR). We argue that the extra cost stems from the inconsistency between the detector and the generative model, along with redundant generation. We exclude inconsistent generators by inverting the original detector, eliminating the necessity of training or saving generative models. We simplify redundant generation by augmented replay to reuse the objects in generated samples, thus reducing the demand for the generated samples. This way, we can generate satisfactory samples in only a few minutes. To effectively utilize the generated objects, we distill the incremental data containing replayed generated objects. However, the generated objects are overwhelmed by the background, leading to ineffective distillation. We propose high-response knowledge distillation to focus on distilling outputs that are more relevant to old classes. Additionally, with the addition of the generated objects and losses, we observe a bias towards old classes in the detector. To alleviate the bias, we balance the losses relative to old and new classes.

The contributions of our works can be summarized as follows:

- To compensate for the absence of old-class objects at a computational low cost, we inverse the original detector to generate old-class samples and reuse the objects in generated samples by augmented replay. To our knowledge, this is the first work generating objects by inverting the detector in the IOD.
- To effectively utilize the generated objects, we propose high-response distillation to focus on information relevant to the old classes. We also balance the losses for old and new classes to trade off stability and plasticity, thereby increasing the overall detection accuracy.
- Extensive experiments on MS COCO 2017 demonstrate that the proposed method achieves state-of-the-art performance in non co-occurring IOD.

2 Related Work

Incremental learning: Incremental learning aims to study catastrophic forgetting [24], i.e., forgetting old knowledge while learning new knowledge. Incremental learning methods have been extensively studied in image classification [5] and can be divided into regularization-based, parameter-isolation-based, and replay-based methods. Regularization-based methods introduce constraints on important parameters [15] or use distillation to consolidate learned knowledge [18]. LwF [18] is a typical example of constrained features and the first method that introduces knowledge distillation into incremental learning. Parameter-isolation-based approaches learn task-specific parameters for different tasks by adding extra model branches during incremental learning [13, 33]. These methods require a task ID for accurate activation, but this information is only available in task incremental learning. Replay-based methods store subsets of old samples in various forms, which require fixed or expandable memory [32, 27]. However, these methods cannot be generalized in all scenarios due to the limited storage space. Therefore, generating pseudo-old class samples is proposed as another replay-based method [29]. Generative Adversarial Networks [9] and Diffusion Model [12] have been introduced into incremental learning as typical generative methods. However, these methods must train and save generative models about old classes, which require additional costs. In contrast, DeepInversion [35] generates old-class objects with similar activations to the old training data. This approach eliminates the need for additional training and saving of the generated model and thus has the potential to be applied in more incremental learning scenarios.

Object detection: Detector networks can be categorized into two-stage anchored, single-stage anchored and anchor-free detectors [37]. Two-stage anchored detectors has the best detection accuracy but is slower to detect, such as Faster R-CNN [28]. Single-stage anchored detectors are faster, but the fusion of stages leads to accuracy degradation. Some methods mitigate the accuracy degradation, such as Retinanet [20] by redesigning the loss function to mitigate the imbalance between foreground and background. In practice, anchor-based detectors need to set many hyper-parameters about anchors, which brings inconvenience. Hence, the anchor-free detector is proposed. GFL re-explores the inconsistent and inflexible representations of the prediction branch and designs a more accurate way of predicting the distribution [17]. So far, anchor-free detectors have achieved state-of-the-art accuracy and speed. In this work, we extend GFL to enable it to learn new classes incrementally.

Incremental Object Detection(IOD): Most of the existing incremental object detection methods use knowledge distillation to transfer knowledge from the original model to the incremental model. [30] using knowledge distillation to normalize the outputs of the classification and regression layers in the detection head, which was the first incremental object detection method. Since then, many researchers have focused on designing different distillation methods. ERD [8] focuses on utilizing statistics for selecting high-response locations to effectively transfer knowledge from old models. Compared to incremental classification tasks, distillation-based methods have higher accuracy gains in incremental object detection tasks. The accuracy gains are due to the possibility that unlabeled old-class objects may exist in the new scene, and distillation-based methods can effectively mine the information of unlabeled old-class objects. However, for some scenes with sparse objects, old-class objects may not exist in the new scene, which leads to a rapid accuracy degradation for distillation-based methods [34]. Therefore, some methods expect to guarantee the generality of IOD by saving some old-class samples or objects. ABR [23] investigates the foreground shift problem that IOD encounters when preserving old-class samples and solves the problem by cutting and preserving old-class objects. Although these methods have good accuracy in all kinds of IOD scenarios, they face failure in cases where the real old-class data is inaccessible. Therefore, some methods expect to increase the IOD accuracy by generating the old-class data. PseudoRM [34] uses generators to generate old-class samples and paste the old-class samples into the new training data. However, these methods require significant additional costs to train the model and generate samples, so there are limitations to the application.

3 METHOD

3.1 Overview

Most existing distillation-based IOD underperform when unlabeled old-class objects are absent in the incremental dataset. In this paper, we generate old-class objects at low cost and utilize the generated

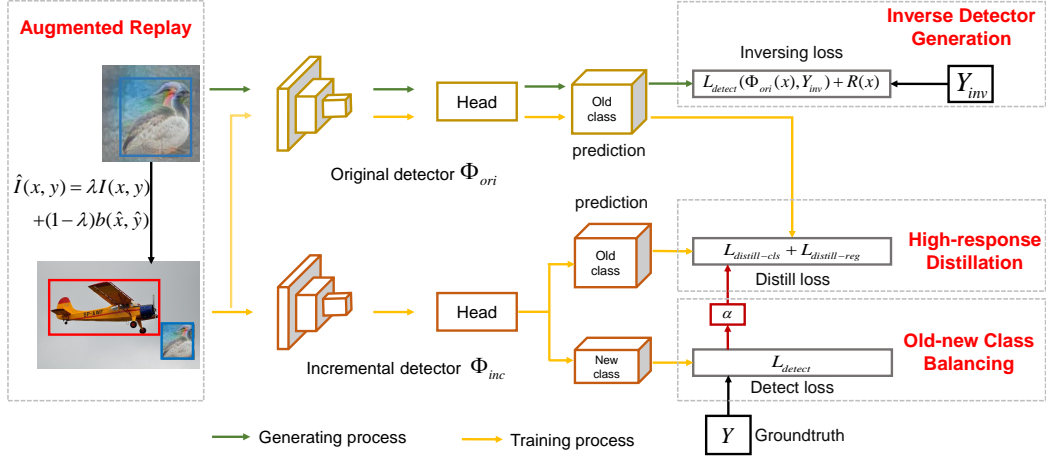


Figure 2: Framework of efficient generated objects replay for incremental object detection

objects to effectively mitigate the performance degradation due to the absence of old-class objects. Fig. 2 illustrates the entire framework. For generating old-class objects at low cost, we generate old-class objects by inverting the original detectors to eliminate the necessity of training and storing additional generative models. Moreover, We augmently replay the generated old-class objects in incremental data, thus reducing the requirement for generating objects. For effectively utilizing the generated objects, we propose high-response knowledge distillation to focus on high-value information. We also trade off stability and plasticity by balancing the loss related to the old and new classes, improving overall accuracy.

3.2 Inverse Detector Generation

Existing generation-based IOD approaches often require extra generative models. However, the inconsistency between the extra generative model and the detector has pitfalls. The direct effect of the inconsistency is the extra training cost incurred by the generative model. In this section, we invert the detector to generate old class objects to eliminate this inconsistency.

Detector inverting. Given a batch of B input generated images $x_{inv} \in B \times C \times W \times H$ and the original detector $\Phi_{ori}(x)$, we formulate inverting the original detector as a regularized minimization problem that each pixel initialized from a random noise $x_{b,c,w,h} \sim N(0, 1)$ and optimizes,

$$x_{inv} = \min_x L_{detect}(\Phi_{ori}(x), Y_{inv}) + R(x) \quad (1)$$

where L_{detect} is the loss function between the prediction of the original detector and the sampled label Y . This loss function is the same as the detection loss of the selected detector and is responsible for determining the category and position of the synthesized object in x_{inv} . In this work, L_{detect} consists of three parts: a classification loss L_{cls} , a center-ness loss L_{cen} , and a regression loss L_{reg} , which are the same as the detection loss in GFL. The sampled label Y_{inv} consists of five parameters, an object category c and four object bounding coordinates x , y , w , and h , which is generated by a bounding box Sampler.

To generate images closer to the real one, we use R to regularize the optimization process. R consists of two parts, a prior term R_{prior} that restricts image priors [2], and a regularization term R_{BN} that regularizes feature map statistics [2]:

$$R(x) = R_{prior}(x) + R_{BN}(x) \quad (2)$$

The combination of R_{prior} and R_{BN} pushes the distribution of generated images closer to real images. It is worth noting that we observe that the reality of the generated objects is insignificant to IOD. The insignificance may be because IOD can learn real image distributions from the backgrounds in incremental data. Thus, the category-related information associated with L_{detect} is more significant. We will analyze the conclusion more in the experimental section.

Histogram-based Bounding Box Sampler. The old-class label information is not available in IOD, and the label Y_{inv} matching the real old-class distribution is essential for generating high-quality

objects. Therefore, we propose a histogram-based bounding box sampling strategy to sample the label Y_{inv} automatically.

To preserve the real label statistics, we additionally preserve the histograms of the real object’s aspect ratios of each class. When generating the objects, a label Y_{inv} is sampled for each generated image $x_{inv} \in B \times C \times W \times H$. In label Y_{inv} , c is the desired class of objects; the position x, y, w is determined by a uniform distribution; the position $h = w \times ratio$, where $ratio$ is sampling from the preserved histogram. In this way, we can ensure that the generated object has a consistent aspect ratio with the real object, resulting in more actual generation.

3.3 Augmented Replay

Redundant generation is another factor that brings extra computational cost. We expect to reduce the redundancy by reusing generated objects. We expect to reduce the redundancy by reusing generated objects. In this section, we crop out the objects in the generated samples and augmently replay the generated object to incremental data. Our approach can achieve satisfactory accuracy with only a few generated objects.

To reuse the generated old-class objects, we crop the objects from the generated images based on the bounding boxes and repeatedly place them in the incremental data. The placing process expects to make the objects naturally fit into the image while minimizing the overlap between the bounding boxes of the objects.

Given an image $I \in C \times W \times H$ which has several groundtruth bounding boxes g and a cropped bounding box b . We assign a random location in image I for cropped bounding box b . Motivated by [36], we then mix b with I to create a new image \hat{I} . Specifically, \hat{I} is obtained by weighted summation of b and I with a mixing coefficient λ . For each pixel (x, y) in \hat{I} , the mixed pixel value is computed by:

$$\hat{I}(x, y) = \begin{cases} \lambda I(x, y) + (1 - \lambda)b(\hat{x}, \hat{y}), & \text{if } g \cup b \leq thr \\ I(x, y), & \text{otherwise} \end{cases} \quad (3)$$

where mixing coefficient λ is in the range $[0, 1]$ and is sampled from the Beta distribution; $b(\hat{x}, \hat{y})$ is a cropped bounding box with a randomly assigned location; $g \cup b$ is the Intersection over Union (IOU) between each g and b ; thr is a threshold value. If the maximum IOU between each g and b is less than or equal to thr , then the pixel value $\hat{I}(x, y)$ is a mixture of the original pixel value $I(x, y)$ and the corresponding pixel value in the cropped bounding box b . If the maximum IOU between a given g and b is greater than thr , then the location of the $b(\hat{x}, \hat{y})$ requires reassignment. Note that we set an upper limit on the assignment iteration since the groundtruth bounding box g may occupy most of the image I , resulting in no locations available for assignment satisfying $g \cup b \leq thr$. Moreover, several b can be replayed in an image I to better reuse the generated objects.

3.4 High-response Distillation

In this section, to effectively utilize the generated objects, we distill the head of the detector. We observe that distilling all the responses in the head leads to a degradation in accuracy, so we select the high responses for distillation. The overall learning target of the incremental detector is defined as:

$$L_{total} = L_{detect} + L_{distill-cls} + L_{distill-reg} \quad (4)$$

where the loss term L_{detect} is the detector-specific classification and regression loss to train incremental detectors for detecting new-class objects. The second loss term $L_{distill-cls}$ is the incremental classification distillation loss for the classification head. The third loss term $L_{distill-reg}$ is the incremental regression distillation loss for the regression head. Notably, since the original detector has only the output for the old class, both $L_{distill-cls}$ and $L_{distill-reg}$ are used for the old-class output in the head. In the following, we describe the high-response distillation for the baseline detector GFL [17].

High-response Distillation at Classification Head. The soft predictions from the classification head contain knowledge of categories learned by the original detector. In this work, we use the $L2$ loss to distill the classification head outputs without the activation function due to the compression of the category information by the sigmoid activation. Furthermore, previous work typically utilizes all predicted responses from the classification head and treats each position equally. However, this

strategy results in the responses generated by the background overwhelming the responses generated by the foreground, thus interfering with transmitting old knowledge. Therefore, we select the top-K highest response to calculate the distillation loss. The distillation loss at the classification head can be described as:

$$L_{distill-cls} = \sum_{k=1}^K (\Phi_{ori-cls}(x_{mix})^k - \Phi_{inc-cls}(x_{mix})^k)^2 \quad (5)$$

Where $\Phi_{ori-cls}(x_{mix})^k$ is one of the top-K selected responses from the original detector’s classification head; $\Phi_{inc-cls}(x_{mix})^k$ is corresponding responses from incremental detector’s classification head. By high-response distillation, more valuable old-class information is transferred to the incremental detector.

High-response Distillation at Regression Head. The location predictions from the regression head are also significant for IOD. In previous detectors, location predictions from the regression head were modeled as delta distributions [22]. The predictions of this modeling approach do not contain confidence information, so locations without objects output incorrect location predictions. Therefore, previous detectors tend to discard the distillation in the regression head. However, GFL uses a vector to represent the arbitrary distribution of box locations. Instead, GFL uses a vector to represent the arbitrary distribution of box locations, which can represent the uncertainty of location prediction [17]. In this way, the high response in the regression head represents the reliable location prediction. Thus, distilling high response in the regression head can effectively transfer the location information from the generated objects.

GFL separately represents the four boundaries location L as probability distribution via the SoftMax function. Thus, the output through SoftMax is utilized to compute the distillation loss. We utilize KL-Divergence loss distilling top-K high-response prediction,

$$L_{distill-reg} = \sum_{l \in L} \sum_{k=1}^K L_{KL}^l(\Phi_{inc-reg}(x_{mix})^k - \Phi_{ori-reg}(x_{mix})^k) \quad (6)$$

Where $\Phi_{ori-reg}(x_{mix})^k$ is one of the top-K selected responses from original detector’s regression head; $\Phi_{inc-reg}(x_{mix})^k$ is corresponding responses from incremental detector’s regression head; L_{KL}^l is KL-Divergence distillation loss for one of the boundary location l . By high-response distillation, more valuable location information is transferred to the incremental detector.

3.5 Old-new Class Balancing

In this section, we propose the old-new class balancing method to balance the stability and plasticity of the incremental detector. We observe that although the old-class-related distillation loss effectively retains the old-class knowledge, it also reduces the detector’s ability to learn new-class knowledge. Therefore, we expect to down-weight old-class-related loss when the detector learns new-class knowledge with hardness. Meanwhile, we up-weight old-class-related loss when the detector can easily detect the new-class object.

Motivated by [20], we use the detector’s estimated probability for positive new-class examples to evaluate the performance in learning new-class knowledge. We propose a modulating factor $\alpha \in [0, 1]$ to balance the loss related to old and new classes, which can be described as:

$$\alpha = \left(\sum_{n=1}^N \frac{p_n}{N} \right)^\gamma \quad (7)$$

Where N denotes the number of positive new-class examples in a batch; p_n is one of the estimated probabilities for positive new-class examples; γ is a tunable parameter with $\gamma \geq 0$.

We balance the detection loss and distillation loss by the modulating factor α , which can be described as:

$$L_{total} = L_{detect} + \alpha (L_{distill-cls} + L_{distill-reg}) \quad (8)$$

When the detector has difficulty detecting new-class objects, the distillation loss weights are down-weighted. Conversely, when the detector easily detects new-class objects, the distillation loss weights are up-weighted. In this way, the detector can dynamically weigh losses during incremental learning, thus improving overall accuracy.

Table 1: Comparisons between state-of-the-art incremental detectors on MS COCO 2017 dataset under different scenarios.

Setting	Method	Base Model	40+40	50+30	60+20	70+10
Co-occurring	Upper Bound	GFL	39.0	39.0	39.0	39.0
	Catastrophic Forgetting	GFL	17.4	13.4	9.1	3.3
	RILOD [16]	Retinanet	29.9	28.5	25.4	24.5
	SID [26]	FCOS	34.0	33.8	32.7	32.8
	ERD [8]	GFL	36.9	36.6	35.8	34.9
	PesudoRM [34]	Faster R-CNN	25.3	-	-	-
	EGOR (our)	GFL	35.5	35.8	36.3	35.9
Non Co-occurring	Upper Bound	GFL	34.4	34.1	34.2	36.6
	Catastrophic Forgetting	GFL	12.3	8.6	4.5	1.4
	ERD [8]	GFL	27.2	27.3	26.9	25.5
	PesudoRM [34]	Faster R-CNN	24.7	-	-	-
	EGOR (our)	GFL	29.2	28.8	27.6	29.9

4 Experiments

4.1 Experimental Settings

Datasets and Evaluation metrics. We evaluated the proposed method on the publicly available dataset MS COCO 2017 [21]. MS COCO 2017 is a challenging object detection dataset containing 80 object classes. In our experiments on this dataset, we use the train2017 set for training and the val2017 set for testing. For the evaluation metric, we report the mAP at different IOUs ranging from 0.5 to 0.95 IoU (mAP@[50:95]).

IOD Setting. To better evaluate the impact of the real old-class objects in the incremental data, we set up two versions of the incremental dataset, the non co-occurring and the co-occurring setting. In the non co-occurring setting, we put the data, including both old and new class objects, into the original dataset only, and the incremental dataset excludes the old-class objects. On the other hand, in the co-occurring setting, we put data with both old and new class objects in both the original and incremental datasets, which means the incremental dataset contains unlabeled real old-class objects. We verify the effectiveness of our method in co-occurring and non co-occurring setting, respectively.

Implementation Details. We use GFL [17] as the basic object detector, which uses ResNet-50 [11] as its backbone and FPN [19] as its neck. Resnet-50 [11] is a pre-trained model on ImageNet [6] and completely freezes batch norm layers [14] during training. The optimizer is set up as the original paper. The framework of our method is implemented on mmdetection [3]. All experiments were performed on an NVIDIA GeForce RTX 4090 with a batch size of 8.

4.2 Overall Performance

In this section, we evaluate the performance of adding new categories at once. The results are reported in Table 1 for different settings. We observe that when the old-class detector is fine-tuned directly using the new data, the AP decreases significantly in all settings. This is because after fine-tuning, the detector’s AP for the old-class object approaches 0, leading to catastrophic forgetting. EGOR far outperformed the fine-tuning method in all settings. Specifically, the AP of EGOR improves by 16.9% and 19.5% in the non co-occurring and co-occurring scenarios with the category "40+40", respectively, and also improves significantly in all other settings, which indicates that EGOR can well address the catastrophic forgetting problem.

Furthermore, we compare EGOR with RILOD [16], SID [26], ERD [8] and PesudoRM [34]. For the co-occurring scenario, the results of all other methods are obtained from the paper [8]. For the non co-occurring scenario, the ERD [8] publishes the code, and we run the code to get the results. PesudoRM publishes the performance for the non co-occurring scenario, and we directly refer to the results in the paper. EGOR achieves state-of-the-art performance in all non co-occurring scenarios, significantly improving performance. Compared to ERD’s distillation-only, EGOR generates old-class objects that provide old-class information for distillation, thus alleviating the forgetting of old-class knowledge. Compared with PesudoRM [34], which generates old-class samples through additional generators,

Table 2: Ablation study based on GFL under first 40 classes + last 40 classes.

Distillation	High-response Distillation	Augmented Replay	Histogram-based Sampler	Old-new class Balancing	Old-class mAP	New-class mAP	Total mAP
✓					33.7	19.0	26.4
✓	✓				32.0	20.2	26.1
✓		✓	✓		33.3	19.1	26.2
✓	✓	✓	✓		37.8	19.9	28.9
✓	✓	✓			37.2	19.8	28.5
✓	✓	✓	✓	✓	38.0	20.3	29.2

γ	Old-class mAP	New-class mAP	Total mAP
0	37.8	19.9	28.9
0.5	38.0	20.3	29.2
1	36.8	21.2	29.0
1.5	34.5	21.9	28.2
2.0	34.0	22.2	28.1

Table 3: Varing γ for old-new class balancing.

Amount	Old-class mAP	New-class mAP	Total mAP
1	37.3	20.5	28.9
3	37.3	20.3	28.8
10	37.9	20.2	29.1
30	38.0	20.4	29.2
100	37.6	20.2	28.9

Table 4: Varing amounts of generated objects.

EGOR eliminates additional generator training and reuses generated objects, thus complementing the absence of old-class objects at a low cost. Moreover, EGOR also shows good performance in the co-occurring scenario.

4.3 Analysis and Ablation Study

To evaluate the performance of the proposed Efficient Generated Objects Replay on the non co-occurring dataset, we conduct experiments on MS COCO 2017. Table 2 evaluates each component on the "40+40" setting. To better illustrate the impact of different components on performance, we publish the first 40 classes, the last 40 classes, and the total mAP, respectively. The method in the first line of Table 2 only distills incremental data without additional generated objects. While mitigating catastrophic forgetting partially, this method has poor accuracy due to the absence of old-class objects in the non co-occurring scenario. After adding high-response distillation, the method results in a further 1.7% performance degradation of the old class due to the lack of high-response outputs in the non co-occurring scenario. The third row lists the results after augmently replaying the generated objects. It can be observed that there is no significant change since the generated object's response is interfered with the background response. After adding high response distillation, the old-class mAP noticeably increases 4.5% by accurately distilling the response of the generated object. This improvement suggests that the generated objects can effectively complement the absence of real objects, thus alleviating catastrophic forgetting. The fifth line deletes histogram-based bounding box Sampler when generating the old-class object, resulting in a 0.6% decrease of the old class. This result suggests that histogram-based bounding box Sampler can increase the old-class information contained in the generated object. The sixth row shows the result of adding old-new class balancing, which increases the total mAP by 0.3%, indicating that the method can improve overall accuracy by better balancing the stability and plasticity.

Tunable Parameter γ . We conduct experiments in the non co-occurring scenario under the "40+40" setting to investigate the effect of the parameter gamma, which is utilized to adjust the modulating factor in old-new class balancing. Table 3 compares the results under gamma values of 0, 0.5, 1, and 1.5. We observe that at value of 0.5, the mAP of both the old and new classes is improved.

4.4 Experiments on generating efficiency

In this section, we demonstrate the efficiency of EGOR by comparing the accuracy for different generated amounts and inverting loss. Moreover, we provide the practical runtimes of generating objects.

Requirement of Generated Object. To investigate the requirement of the generated object, we compare the mAP with different amounts of generated objects in the non co-occurring scenario under the “40+40” setting. Each generated object is repeatedly replayed to the incremental data. Table 4 lists the results under different amounts of generated objects. We observe that the maximum total map gap is merely 0.3%, which indicates that generating few objects can efficiently complement the absence of old-class objects. Thus, the proposed method can improve the IOD performance in the non co-occurring scenarios with low cost.

inversing Loss. To investigate the effect of different inversing losses, we compare the mAP at each loss in the non co-occurring scenario under the “40+40” setting. In inversing losses, L_{detect} is used to guide the object category, and R_{BN} and R_{prior} are used to make the object more natural. It’s worth noting that combining more losses slows the convergence, thus requiring more

training iteration. The first line uses only L_{detect} and converges after 500 iterations. The fourth row in Table 5 utilizes all inversing losses and converges after 2000 iterations. Upon comparison, we observe that the degradation is only 0.4% in the total map after removing R_{BN} and R_{prior} , which indicates that the proposed method requires more category information than the information of the natural image distribution. The results differ from the conclusion in classification tasks [] that the generated objects’ domain bias seriously affects the incremental learning performance. The distinctions may be because the background in the IOD incremental data can provide rich information related to real-image distribution. Therefore, the generated objects only need to focus on the category-related information without mimicking the real-image distribution. To generate the old-class objects more efficiently, we can inverse the original detector using only L_{detect} , which reduces the generation cost to a quarter.

Realistic Generation Speed. To illustrate the effectiveness of the proposed EGOR at minimal cost, we conduct experiments in the non co-occurring scenario under the “40+40” setting. We generate the old-class objects in 2.5 minutes on an NVIDIA GeForce RTX 4090. Compared to the 12 hours of incremental training, the extra 2.5 minutes is negligible. As shown in Fig. 3, the old-class accuracy of EGOR increases 3.8% and the overall accuracy of EGOR increases 2.2%, proving the EGOR efficiently mitigates catastrophic forgetting in the non co-occurring scenarios.

5 Conclusion

In this paper, we propose Efficient Generated Objects Replay (EGOR) to low-costly mitigate the accuracy degradation of distillation-based IOD in non co-occurring incremental data. To efficiently complement the absence of old class objects, we generate old class objects by inversing the original detectors without the requirements of training and storing extra generative models. Furthermore, we propose augmented replay to reuse the generated objects, thus reducing the generation requirements. To effectively exploit the generated objects, we propose high-response knowledge distillation to mitigate the interference of the background on the generated objects. Moreover, with additional generated objects and losses, we observe a tendency for the detector to be biased towards old classes. To mitigate this bias, we balance the losses relative to the old and new classes during training, thereby improving the overall detection accuracy. Extensive experiments validate the efficiency and effectiveness of EGOR.

Table 5: The effect of different inversing loss.

L_{detect}	R_{BN}	R_{prior}	Old-class mAP	New-class mAP	Total mAP
✓			37.5	19.9	28.8
✓	✓		37.7	20.1	28.9
✓		✓	37.8	19.9	28.9
✓	✓	✓	38.0	20.3	29.2

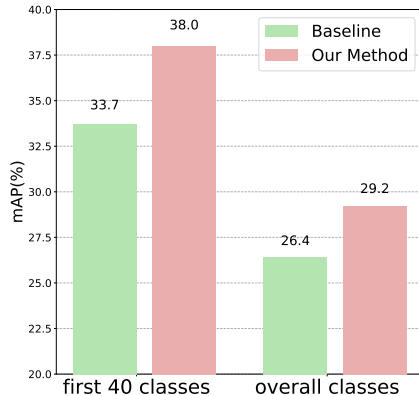


Figure 3: Accuracy of the proposed EGOR at minimum generating cost. EGOR generates one object per class with 500 iterations, taking only 2.5 minutes by an NVIDIA GeForce RTX 4090.

References

- [1] Fabio Cermelli et al. “Modeling missing annotations for incremental learning in object detection”. In: *Proceedings of the IEEE/CVF Conference on Computer Vision and Pattern Recognition*. 2022, pp. 3700–3710.
- [2] Akshay Chawla et al. “Data-free knowledge distillation for object detection”. In: *Proceedings of the IEEE/CVF Winter Conference on Applications of Computer Vision*. 2021, pp. 3289–3298.
- [3] Kai Chen et al. “MMDetection: Open MMLab Detection Toolbox and Benchmark”. In: *arXiv preprint arXiv:1906.07155* (2019).
- [4] Bo Cui, Guyue Hu, and Shan Yu. “RT-Net: replay-and-transfer network for class incremental object detection”. In: *Applied Intelligence* 53.8 (2023), pp. 8864–8878.
- [5] Matthias De Lange et al. “A continual learning survey: Defying forgetting in classification tasks”. In: *IEEE transactions on pattern analysis and machine intelligence* 44.7 (2021), pp. 3366–3385.
- [6] Jia Deng et al. “Imagenet: A large-scale hierarchical image database”. In: *2009 IEEE conference on computer vision and pattern recognition*. Ieee. 2009, pp. 248–255.
- [7] Na Dong et al. “Class-incremental object detection”. In: *Pattern Recognition* 139 (2023), p. 109488.
- [8] Tao Feng, Mang Wang, and Hangjie Yuan. “Overcoming catastrophic forgetting in incremental object detection via elastic response distillation”. In: *Proceedings of the IEEE/CVF Conference on Computer Vision and Pattern Recognition*. 2022, pp. 9427–9436.
- [9] Ian Goodfellow et al. “Generative adversarial nets”. In: *Advances in neural information processing systems* 27 (2014).
- [10] Ian J Goodfellow et al. “An empirical investigation of catastrophic forgetting in gradient-based neural networks”. In: *arXiv preprint arXiv:1312.6211* (2013).
- [11] Kaiming He et al. “Deep residual learning for image recognition”. In: *Proceedings of the IEEE conference on computer vision and pattern recognition*. 2016, pp. 770–778.
- [12] Jonathan Ho, Ajay Jain, and Pieter Abbeel. “Denoising diffusion probabilistic models”. In: *Advances in neural information processing systems* 33 (2020), pp. 6840–6851.
- [13] Ching-Yi Hung et al. “Compacting, picking and growing for unforgetting continual learning”. In: *Advances in neural information processing systems* 32 (2019).
- [14] Sergey Ioffe and Christian Szegedy. “Batch normalization: Accelerating deep network training by reducing internal covariate shift”. In: *International conference on machine learning*. pmlr. 2015, pp. 448–456.
- [15] James Kirkpatrick et al. “Overcoming catastrophic forgetting in neural networks”. In: *Proceedings of the national academy of sciences* 114.13 (2017), pp. 3521–3526.
- [16] Dawei Li et al. “RILOD: Near real-time incremental learning for object detection at the edge”. In: *Proceedings of the 4th ACM/IEEE Symposium on Edge Computing*. 2019, pp. 113–126.
- [17] Xiang Li et al. “Generalized focal loss: Learning qualified and distributed bounding boxes for dense object detection”. In: *Advances in Neural Information Processing Systems* 33 (2020), pp. 21002–21012.
- [18] Zhizhong Li and Derek Hoiem. “Learning without forgetting”. In: *IEEE transactions on pattern analysis and machine intelligence* 40.12 (2017), pp. 2935–2947.
- [19] Tsung-Yi Lin et al. “Feature pyramid networks for object detection”. In: *Proceedings of the IEEE conference on computer vision and pattern recognition*. 2017, pp. 2117–2125.
- [20] Tsung-Yi Lin et al. “Focal loss for dense object detection”. In: *Proceedings of the IEEE international conference on computer vision*. 2017, pp. 2980–2988.
- [21] Tsung-Yi Lin et al. “Microsoft coco: Common objects in context”. In: *Computer Vision–ECCV 2014: 13th European Conference, Zurich, Switzerland, September 6–12, 2014, Proceedings, Part V 13*. Springer. 2014, pp. 740–755.
- [22] Wei Liu et al. “Ssd: Single shot multibox detector”. In: *Computer Vision–ECCV 2016: 14th European Conference, Amsterdam, The Netherlands, October 11–14, 2016, Proceedings, Part I 14*. Springer. 2016, pp. 21–37.

- [23] Yuyang Liu et al. “Augmented box replay: Overcoming foreground shift for incremental object detection”. In: *Proceedings of the IEEE/CVF International Conference on Computer Vision*. 2023, pp. 11367–11377.
- [24] Michael McCloskey and Neal J Cohen. “Catastrophic interference in connectionist networks: The sequential learning problem”. In: *Psychology of learning and motivation*. Vol. 24. Elsevier, 1989, pp. 109–165.
- [25] Angelo G Menezes et al. “Continual object detection: a review of definitions, strategies, and challenges”. In: *Neural networks* 161 (2023), pp. 476–493.
- [26] Can Peng et al. “SID: incremental learning for anchor-free object detection via selective and inter-related distillation”. In: *Computer vision and image understanding* 210 (2021), p. 103229.
- [27] Ameya Prabhu, Philip HS Torr, and Puneet K Dokania. “Gdumb: A simple approach that questions our progress in continual learning”. In: *Computer Vision—ECCV 2020: 16th European Conference, Glasgow, UK, August 23–28, 2020, Proceedings, Part II 16*. Springer. 2020, pp. 524–540.
- [28] Shaoqing Ren et al. “Faster r-cnn: Towards real-time object detection with region proposal networks”. In: *Advances in neural information processing systems* 28 (2015).
- [29] Hanul Shin et al. “Continual learning with deep generative replay”. In: *Advances in neural information processing systems* 30 (2017).
- [30] Konstantin Shmelkov, Cordelia Schmid, and Karteek Alahari. “Incremental learning of object detectors without catastrophic forgetting”. In: *Proceedings of the IEEE international conference on computer vision*. 2017, pp. 3400–3409.
- [31] Guido M Van de Ven and Andreas S Tolias. “Three scenarios for continual learning”. In: *arXiv preprint arXiv:1904.07734* (2019).
- [32] Yue Wu et al. “Large scale incremental learning”. In: *Proceedings of the IEEE/CVF conference on computer vision and pattern recognition*. 2019, pp. 374–382.
- [33] Shipeng Yan, Jiangwei Xie, and Xuming He. “Der: Dynamically expandable representation for class incremental learning”. In: *Proceedings of the IEEE/CVF conference on computer vision and pattern recognition*. 2021, pp. 3014–3023.
- [34] Dongbao Yang et al. “Pseudo Object Replay and Mining for Incremental Object Detection”. In: *Proceedings of the 31st ACM International Conference on Multimedia*. 2023, pp. 153–162.
- [35] Hongxu Yin et al. “Dreaming to distill: Data-free knowledge transfer via deepinversion”. In: *Proceedings of the IEEE/CVF Conference on Computer Vision and Pattern Recognition*. 2020, pp. 8715–8724.
- [36] Hongyi Zhang et al. “mixup: Beyond empirical risk minimization”. In: *arXiv preprint arXiv:1710.09412* (2017).
- [37] Zhengxia Zou et al. “Object detection in 20 years: A survey”. In: *Proceedings of the IEEE* 111.3 (2023), pp. 257–276.

A Limitations

One limitation of our framework is to focus on restricted storage scenarios, i.e., original training data cannot be saved. In this scenario, we achieve state-of-the-art efficiency and accuracy. However, in some specific scenarios, the storage restriction is not strict, so storing additional old-class data for incremental learning is possible, resulting in better accuracy. We will continue to improve our approach so that the accuracy improvement brought by generated old-class data can match that of real old-class data.

B Broader Impacts

The Inverse Detector Generation can provide a better understanding of the knowledge learned by the detectors and transfer it to the incremental detectors, which provides a technical basis for the development of lifelong learning. However, the Inverse Detector Generation may introduce some privacy issues due to the visualization of learned knowledge. Moreover, the generated data may be attacked, leading to performance degradation after incremental training, which may cause some security issues. The above two issues can be mitigated by limiting the accessibility during incremental training.

C Visualizations of Inverse Detector Generation

We visually compare the difference between generated samples with losses $L_{detect} + R$ and only L_{detect} , to intuitively illustrate the effect of the two losses.

C.1 Generation Implementation Details

For Inverse Detector Generation with $L_{detect} + R$, we use Adam for optimization (with $\beta_1 = \beta_2 = 0$ and a learning rate of 0.2), and randomly flip, brighten, and jitter the inputs before each forward pass. We synthesize 160×160 images with 2000 updates, using an NVIDIA GeForce RTX 4090. For Inverse Detector Generation with only L_{detect} , we reduce the number of updates to 500 iterations.

C.2 Visualizations of Generated Samples

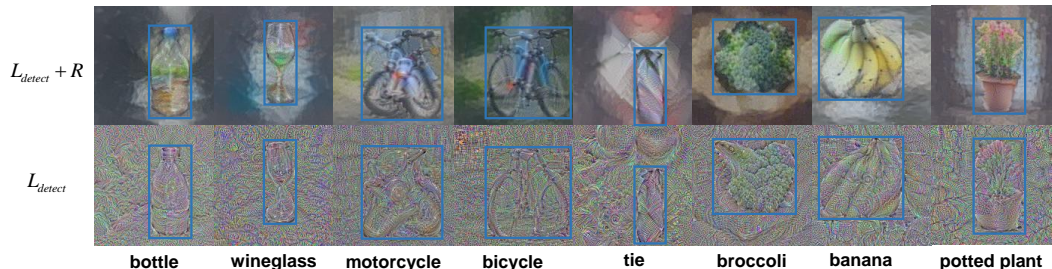


Figure 4: Samples generated by Inverse Detector Generation on the original detector. The sampled label Y_{inv} for each image is represented by a blue box and category label. The first row shows the generated samples utilizing $L_{detect} + R$. The second row shows the generated sample utilizing only L_{detect} .

Fig. 4 shows the samples generated by Inverse Detector Generation utilizing $L_{detect} + R$ and L_{detect} , respectively. We can intuitively observe that utilizing $L_{detect} + R$ allows for the high-quality generation of objects at the sampled label Y_{inv} with reasonable color distribution and clear object contour information. For example, a motorcycle and a bicycle have similar features, but the detector still uncovers subtle differences in wheel and body structure. Therefore, our method can effectively supplement the absence of the old-class objects.

Comparing the generated samples with $L_{detect} + R$ and L_{detect} , we can observe that although the color distribution of the generated samples with L_{detect} differs from the real object. Both the

generated samples with $L_{detect} + R$ and L_{detect} have similar object contour information. In Table 5, there is no significant change in accuracy utilizing $L_{detect} + R$ and L_{detect} , which suggests that object contour information in generated objects is more critical in IOD.

NeurIPS Paper Checklist